

**Utilizing Mathematical Modeling to Simulate
Combination Drug Therapies & Elucidate the
Differential Effects Stromal Fibroblasts Impart on
Breast Cancer Sensitivity to Lapatinib.**

Jonathan Williams

Abstract

1 in 8 women will develop Breast Cancer in their lifetime. Approximately 20% of breast cancers over-express the human epidermal growth factor receptor 2 (HER2) and are deemed HER2+. HER2 targeted therapies selectively target these HER2+ cancer cells and stall breast tumor growth. While HER2 targeted therapies exist, patient response is heterogeneous as between 38% - 75% of patients do not respond. Stromal Fibroblasts are an abundant cell type in the breast tumor microenvironment. It has recently been demonstrated that stromal fibroblasts reduce the efficacy of Lapatinib, a commonly prescribed HER2 targeted therapy, in certain HER2+ breast cancer cell lines in vitro. A HER2+ cell line is deemed “fibroblast-protected” if once co-cultured with stromal fibroblasts, it becomes resistant to Lapatinib assault. A HER2+ cell line is deemed “fibroblast-insensitive” if stromal fibroblast co-culture does not induce Lapatinib resistance. To gain a fundamental understanding of fibroblast-protection, a mathematical model of HER2+ breast cancer was constructed in MATLAB. The model was fit to previously collected PI3K/Akt pathway protein expression data, and overall cell growth data. BT 474 (a fibroblast-protected cell line) and HCC 1954 (a fibroblast-insensitive cell line) were modeled. Parameter Sensitivity Analysis revealed that for the fibroblast-protected BT 474, stromal fibroblasts significantly increased cell sensitivity to pro-growth PI3K/Akt pathway signaling. This contrasted with the fibroblast-insensitive HCC 1954 for which stromal fibroblasts did not significantly affect cell sensitivity to pro-growth PI3K/Akt pathway signaling. In addition to providing a mechanistic understanding of fibroblast-protection, the MATLAB model was extended to simulate how combination drug therapies would arrest cell growth in BT 474 and HCC 1954. Mirroring previously published results, model predictions confirmed a Lapatinib + pAkt Inhibitor combination would only synergize to arrest cell growth in HCC 1954. A Lapatinib + pAkt Inhibitor + Fibroblast Signaling Inhibitor combination is predicted to arrest cell growth most effectively in BT 474.

Introduction

Breast Cancer is an extremely common disease. An American woman has a 12.3% lifetime risk of breast cancer diagnosis, and breast cancer is responsible for the second most female cancer deaths (Gagliato, Jardim, Marchesi, & Hortobagyi, 2016). Approximately 20% of breast cancers over-express the human epidermal growth factor receptor 2 and are deemed HER2+. Because HER2+ breast cancers over express the HER2 receptor, they transmit more pro-growth signaling to the cell. As a result, if left untreated, HER2+ breast tumors grow at a faster rate and are more aggressive than HER2- breast tumors.

Fortunately, the advent of HER2 targeted therapies have dramatically improved patient prognosis. HER2 targeted therapies, such as Lapatinib, selectively bind to the HER2 receptors present on HER2+ breast cancer cells, and block the HER2 receptors from initiating pro-growth signaling.

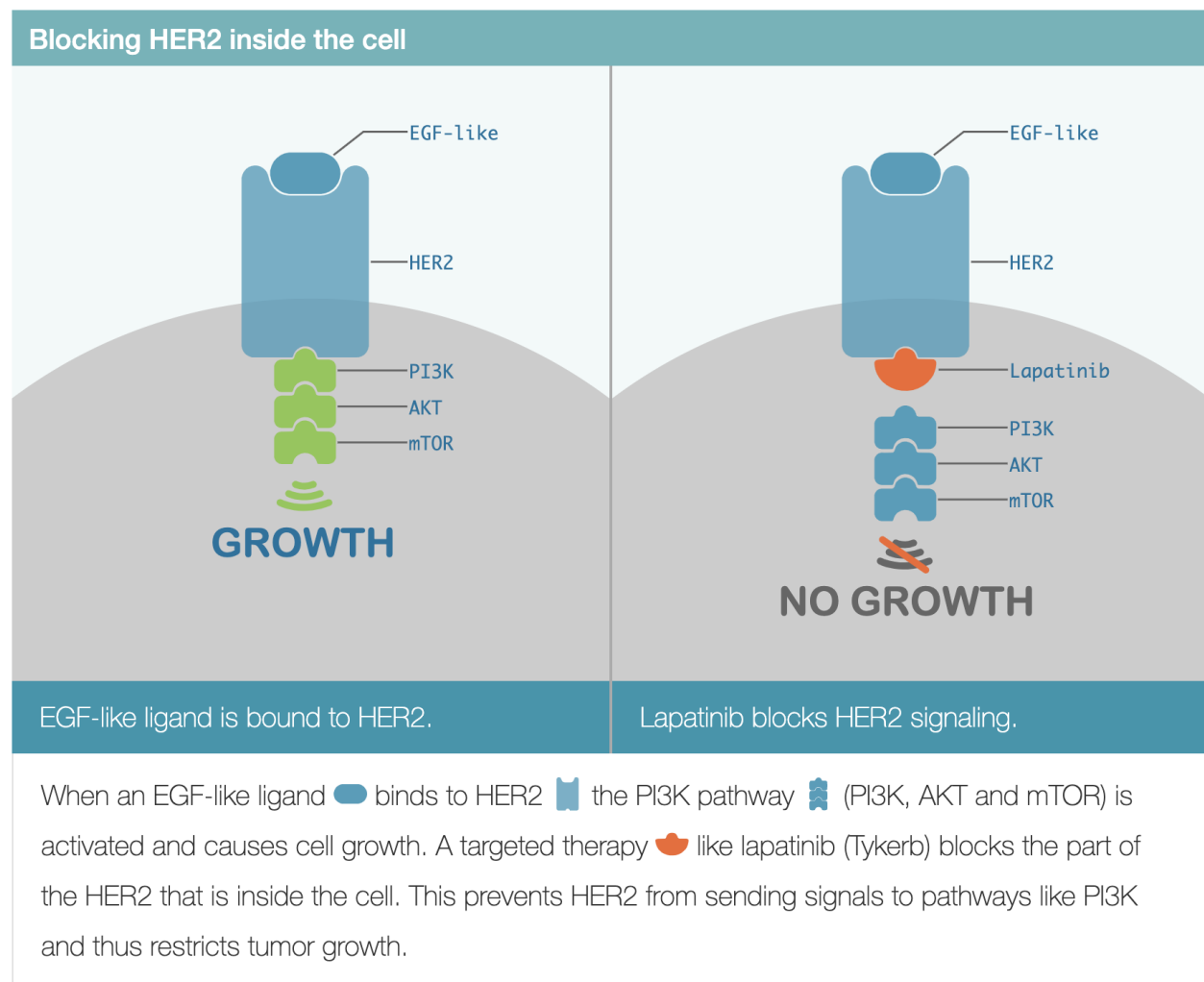


Figure 1: Mechanism of Lapatinib inhibition on pro-growth signaling in HER2+ cells (*HER2 and Targeted Therapy*, 2020)

While HER2 targeted therapies have improved overall prognosis, patient response is variable. Depending on the administered HER2 targeted therapy, 38% - 75% of patients do not respond (Carey et al., 2016).

Investigating mechanisms of resistance to HER2 targeted therapies is a current major vein of breast cancer research.

Stromal Fibroblasts are an abundant cell type in the breast tumor microenvironment. A high density of stromal fibroblasts has been associated with poor survival rates for patients with solid cancers such as breast cancer (Liu et al., 2016). Recently it has been demonstrated that stromal fibroblasts reduce the efficacy of Lapatinib in certain HER2+ breast cancer cell lines in vitro (Zervantonakis et al., 2020). When a “fibroblast-protected” cell line is co-cultured with stromal fibroblasts, they become resistant to the killing effect of Lapatinib. This contrasts to a “fibroblast-insensitive” cell line for which stromal fibroblast co-culture does not impact the killing effect of Lapatinib.

To gain a fundamental understanding of fibroblast-protection, a mathematical model was developed in the programming language MATLAB. The model relates the HER2-initiated signaling cascade of the PI3k/Akt pathway to overall cell growth. The PI3k/Akt pathway was explicitly modeled because it has been implicated with resistance to HER2 targeted therapies (Paplomata & O'Regan, 2014). The model further captures the extracellular influence stromal fibroblasts impart on overall cell growth.

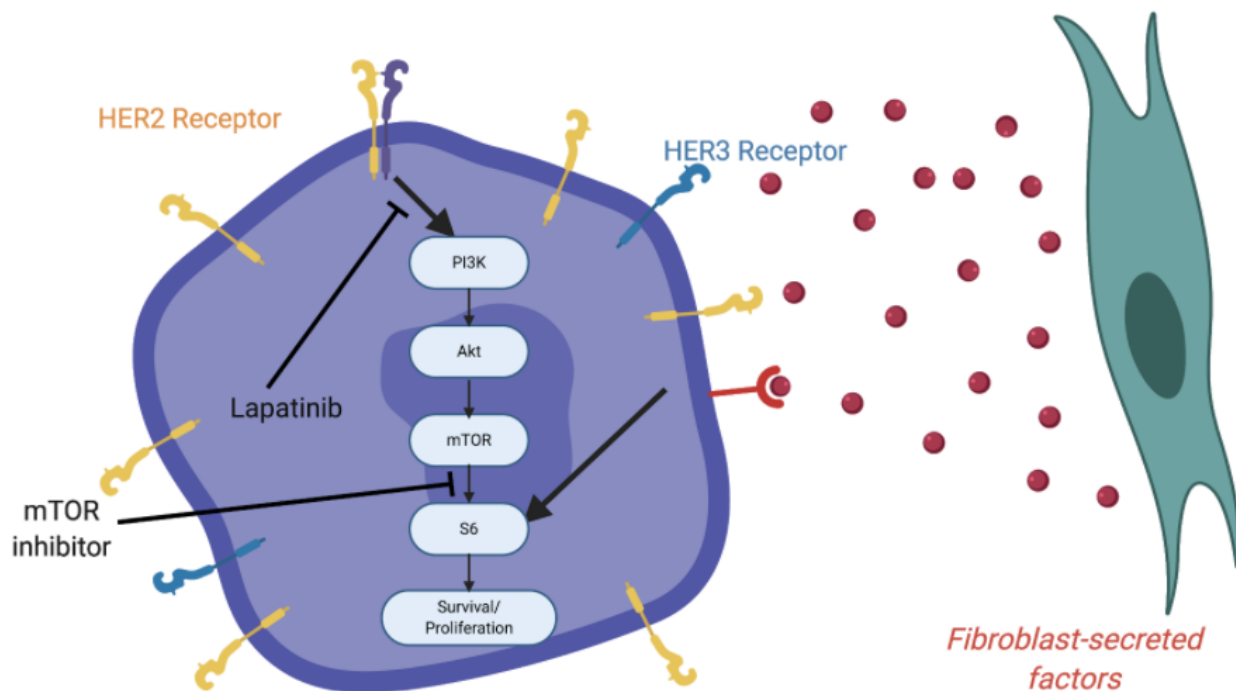


Figure 2: Visual Diagram of the Modeled HER2+ Breast Cancer System (Matthew Poskus)

The model was employed to study the differences between BT 474 (a fibroblast-protected HER2+ cell

line) and HCC 1954 (a fibroblast-insensitive HER2+ cell line). Through performing parameter sensitivity analysis on the BT 474 and HCC 1954 models, the fundamental mechanism of fibroblast-protection from Lapatinib was identified. The MATLAB model was further extended to simulate how combination drug therapies would arrest cell growth in BT 474 and HCC 1954.

Methods

PI3K/Akt Signaling Pathway Importance

The PI3K/Akt signaling pathway regulates breast cancer cell growth and proliferation. The PI3K/Akt pathway is activated once an external ligand binds to a HER2 receptor. Kinases in the pathway activate one another via phosphorylation, and the pathway culminates in downstream kinases activating transcription factors. These transcription factors then regulate pro-growth gene expression.

The PI3K/Akt pathway was included within the mathematical model because it is one of the most commonly mutated signaling pathways present in cancer. Moreover, the PI3K/Akt pathway was included within the model because the pathway has been associated with resistance to HER2 targeted therapies (Paplomata & O'Regan, 2014).

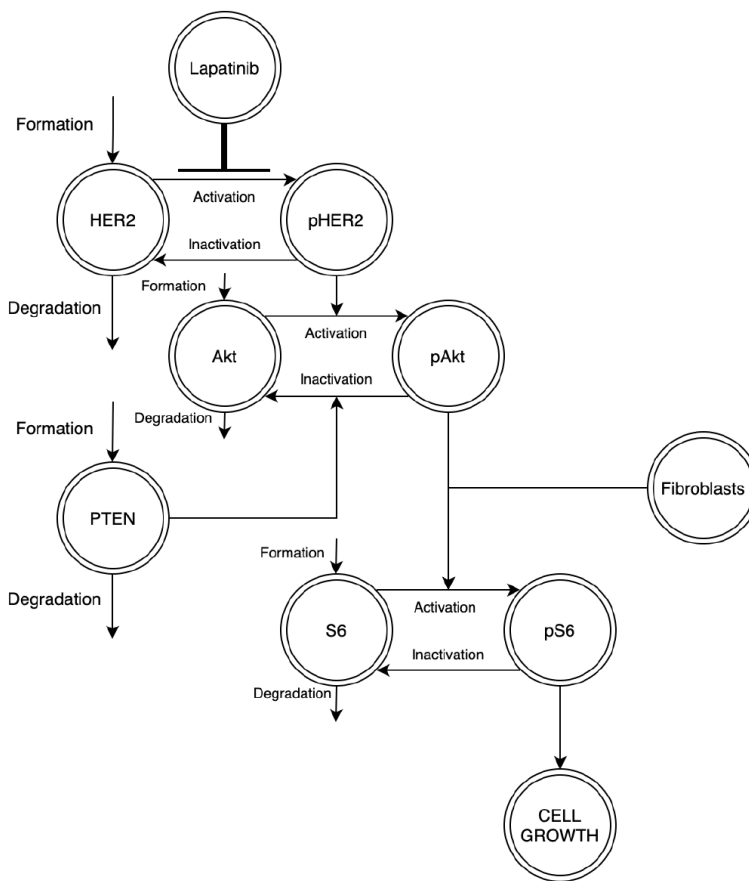


Figure 3: Visual Diagram of Overall Model Topology

The Model abstracts the complex signaling cascade of the PI3K/Akt pathway into interactions between four key proteins. This simplistic representation of the PI3K/Akt pathway was selected to prevent model over-fitting. Three kinases - HER2, Akt, and S6 - are incorporated to represent HER2-initiated signaling directing overall cell growth. A phosphatase - PTEN - is incorporated to represent negative regulation of pro-growth PI3K/Akt pathway signaling. Similar to (Korkola et al., 2015), model links between proteins do not represent direct phosphorylation or dephosphorylation events; rather they represent general interactions for which the intermediary steps are not explicitly described.

S6 is a key downstream regulator of transcription factors involved with cell growth (Dufner & Thomas, 1999). Accordingly, levels of active phosphorylated S6 (pS6) are tied to overall cell growth. To account for fibroblasts aiding cell growth in the face of Lapatinib assault as observed in (Zervantonakis et al., 2020), a fibroblast-mediated route of pS6 activation is incorporated.

BT 474 & HCC 1954 Cell Lines

BT 474 and HCC 1954 were the cell lines to which the model was fit. BT 474 is fibroblast-protected whereas HCC 1954 is fibroblast-insensitive. BT 474 is also PI3k wild type (normal protein function), whereas HCC 1954 is PI3K mutant (abnormal protein function). It should be noted HCC 1954's PI3k mutation is what gives the cell line larger comparative growth than BT 474.

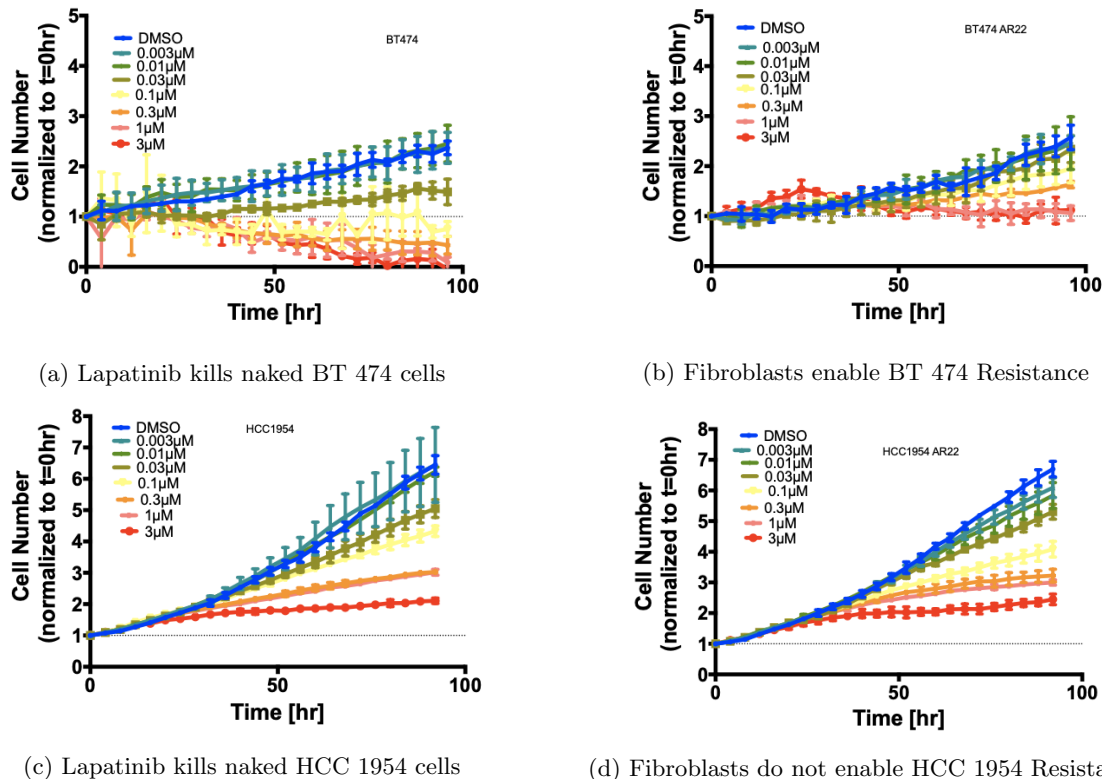


Figure 4: Comparison of Lapatinib efficacy in fibroblast-protected BT 474 vs fibroblast-insensitive HCC 1954. While fibroblast co-culture enables BT 474 resistance to Lapatinib, fibroblast co-culture does not enable HCC 1954 resistance to Lapatinib.

Mathematical Models Generated

Mathematical Models were developed to gain an understanding of how fibroblast co-culture enhanced BT 474 cell growth in the presence of Lapatinib, but did not affect HCC 1954 cell growth in the presence of Lapatinib. Mathematical modeling was employed because by analyzing model parameters, one can numerically quantify differences between BT 474 and HCC 1954 at a specificity unachievable by traditional “wet lab” techniques. Mathematical modeling was further employed because a computational HER2+ breast cancer model could be easily extended to simulate how combination drug therapies would arrest BT 474 and HCC 1954 cell growth.

Four Model variants were generated for analysis:

1. BT 474 under Monoculture & 0.1 μ M Lapatinib Assault
2. BT 474 under Stromal Fibroblast Co-culture & 0.1 μ M Lapatinib Assault
3. HCC 1954 under Monoculture & 0.1 μ M Lapatinib Assault
4. HCC 1954 under Stromal Fibroblast Co-culture & 0.1 μ M Lapatinib Assault

For both BT 474 and HCC 1954, Monoculture and Fibroblast Co-culture model variants were generated to study the influence of stromal fibroblasts on cell growth. All models were simulated under the influence of 0.1 μ M Lapatinib assault. This 0.1 μ M Lapatinib concentration was selected because it was the “borderline” concentration for which stromal fibroblasts first converted a formally cytotoxic response into a continued cell growth response in BT 474 (Figure 4: Images A and B; see yellow growth bar 0.1 μ M Lapatinib).

All mathematical models were formulated using Ordinary Differential Equations (ODEs) which described the rate of change of PI3K/Akt pathway protein concentrations and overall cell growth. Specific ODE terms were derived from chemical kinetic rate laws which described PI3K/Akt pathway protein interactions. Similar to (Kirouac et al., 2017) Lapatinib’s inhibition of the activated HER2 receptor (pHER2) across all models was accounted for by a Hill Equation which incorporated Lapatinib’s 0.1 μ M concentration and IC₅₀ (potency metric). The full set of chemical kinetic rate laws and ODEs employed for each model variant are included in the modeling appendix.

Reverse Phase Protein Array (RPPA) & Cell Viability Data

Reverse Phase Protein Array (RPPA) is a powerful high throughput technique applied to cultured cell samples. Through performing RPPA, the relative concentration (and thus expression) of proteins present in a cell sample are quantified. By providing specific sets of antibodies, one can analyze the entire protein architecture of a cell signaling pathway. To capture how the expression of key proteins in the PI3k/Akt pathway changed over time in BT 474 and HCC 1954, all models were fit to RPPA data collected at 4 and 48 hours. To capture changes in overall cell growth in BT 474 and HCC 1954, all models were fit to cell growth data collected in 4 hour increments for 48 hours. All models were fit to their appropriate RPPA and cell growth data using MATLAB’s lsqnonlin optimization method. The full set of optimized parameter values for each model variant can be found in the modeling appendix.

Results

BT 474 and HCC 1954 ODE Models Accurately Reproduce Experimentally Collected RPPA & Cell Growth Data

The Monoculture and Co-culture BT 474/HCC 1954 ODE models were able to accurately reproduce experimentally collected RPPA and cell growth data. All models were fit to RPPA and cell growth data collected from cultured BT 474/HCC 1954 cells treated with 0.1 μ M Lapatinib. High model accuracy was reflected by the low average root mean squared error (RMSE) of 0.87 across all four models. It should be noted the Monoculture/Co-culture HCC 1954 models were less accurate than the Monoculture/Co-culture BT 474 models (1.492 average RMSE vs 0.25 average RMSE). This accuracy discrepancy arose because the HCC 1954 models were fit to RPPA data collected from separate experimental trials which used slightly different cell seeding protocols.

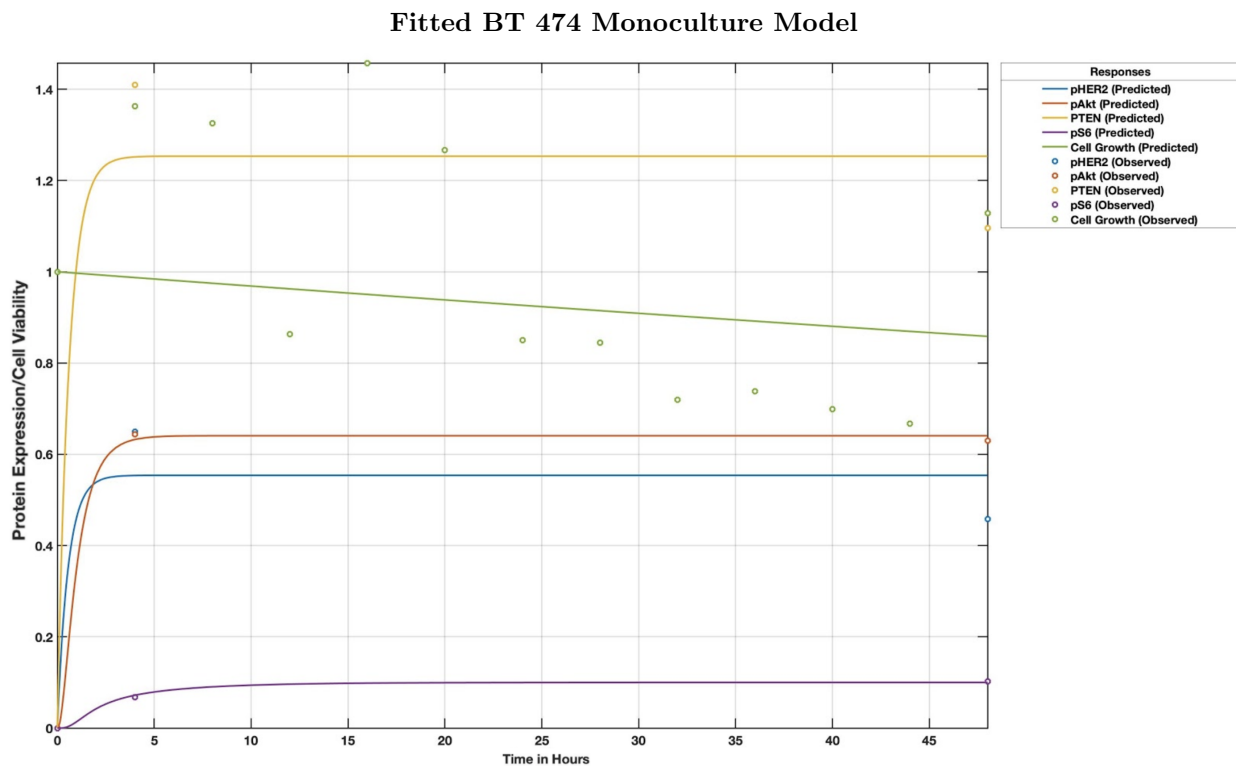


Figure 5: BT 474 Monoculture Model Simulated for 48 hours. Explicit data points are experimentally collected RPPA/Cell Growth data. Solid Lines are optimized model ODE solution curves for respective PI3K/Akt pathway protein species and overall cell growth. Root Mean Squared Error = 0.392

Fitted BT 474 Co-culture Model

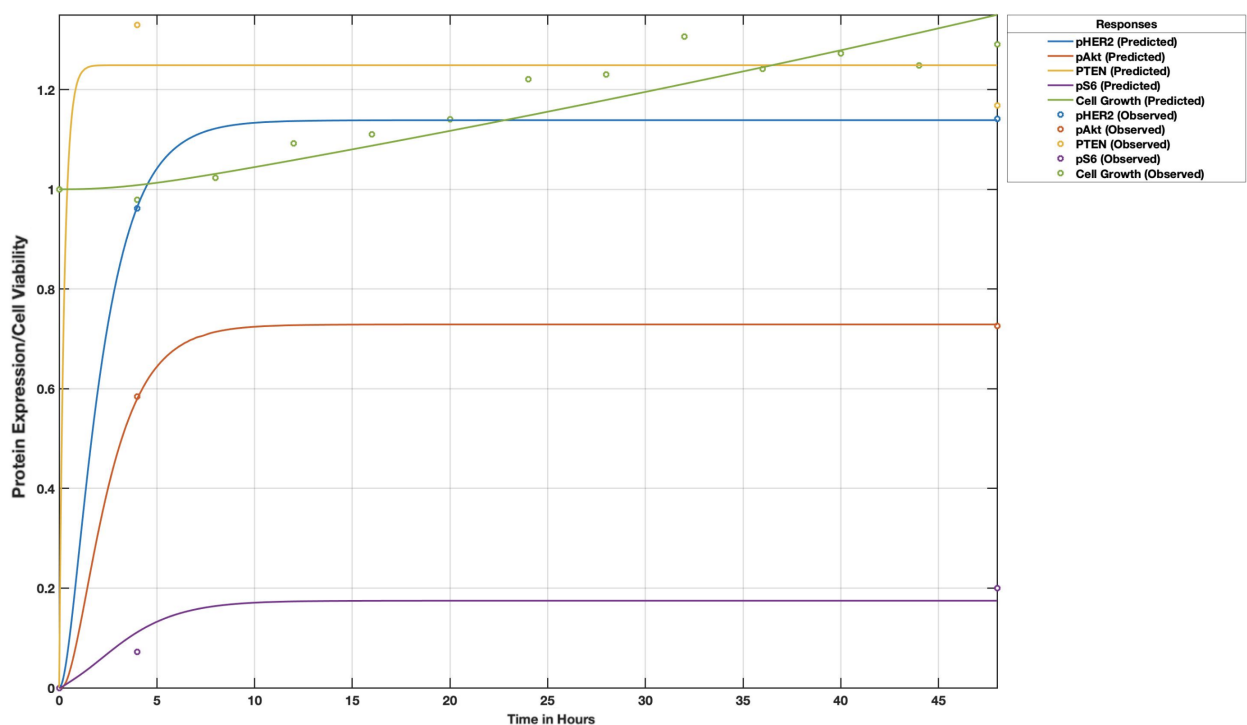


Figure 6: BT 474 Stromal Fibroblast Co-culture Model Simulated for 48 hours. Explicit data points are experimentally collected RPPA/Cell Growth data. Solid Lines are optimized model ODE solution curves for respective PI3K/Akt pathway protein species and overall cell growth. Root Mean Squared Error = 0.104

Fitted HCC 1954 Monoculture Model

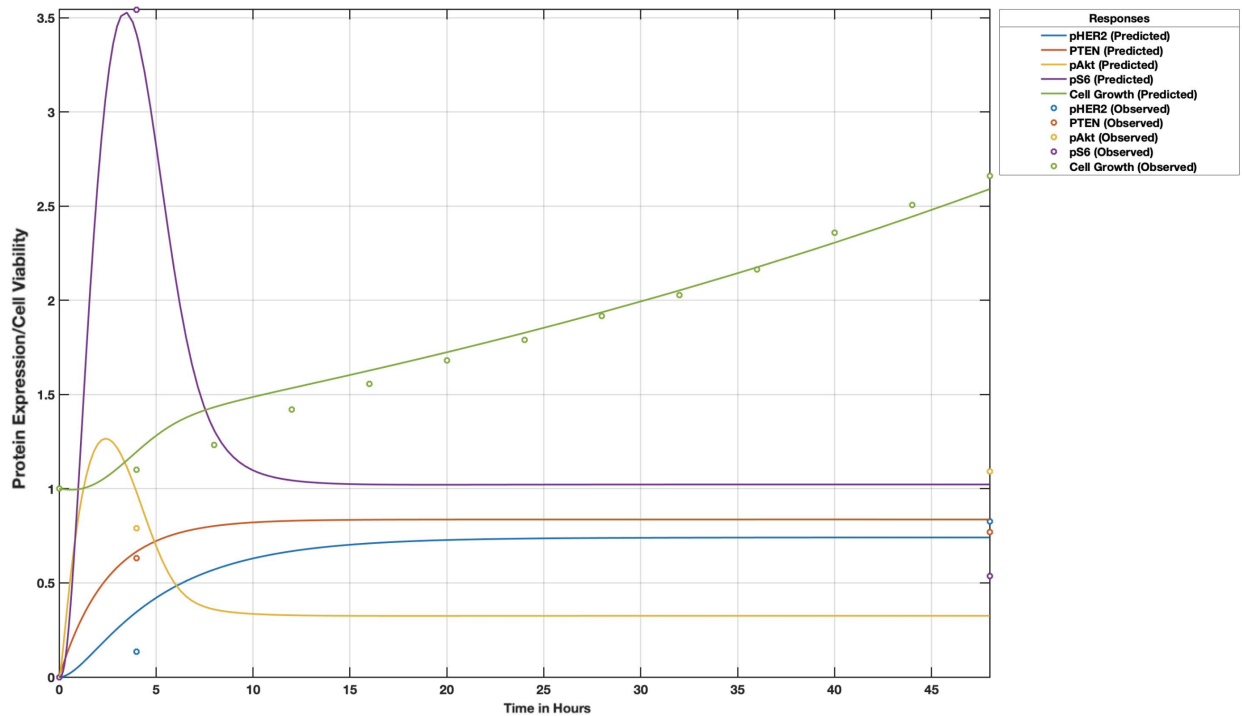


Figure 7: HCC 1954 Monoculture Model Simulated for 48 hours. Explicit data points are experimentally collected RPPA/Cell Growth data. Solid Lines are optimized model ODE solution curves for respective PI3K/Akt pathway protein species and overall cell growth. Root Mean Squared Error = 0.505

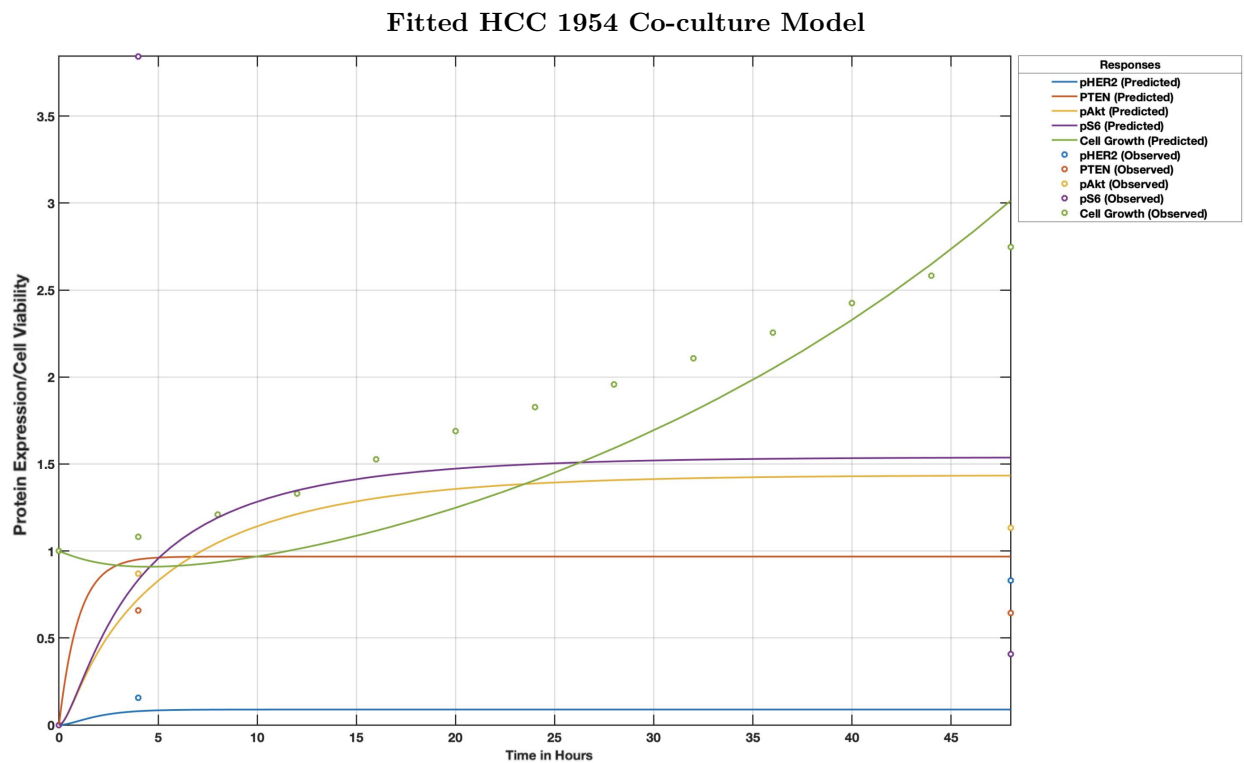


Figure 8: HCC 1954 Stromal Fibroblast Co-culture Model Simulated for 48 hours. Explicit data points are experimentally collected RPPA/Cell Growth data. Solid Lines are optimized model ODE solution curves for respective PI3K/Akt pathway protein species and overall cell growth. Root Mean Squared Error = 2.479

Parameter Sensitivity Analysis Elucidates How Stromal Fibroblasts Differentially Aid the Growth of Fibroblast-Protected Cell Lines

The fitted BT 474/HCC 1954 ODE models accurately replicate observed 48 hour PI3K/Akt pathway protein dynamics and overall cell growth. Now that the complex biology of BT 474 and HCC 1954 had been effectively translated into a mathematical model, parameter sensitivity analysis was conducted to investigate how stromal fibroblasts differentially aided the growth of the fibroblast-protected BT 474 cell line in the face of Lapatinib assault.

In each ODE model, overall cell growth is a multivariate function of the optimized model parameters. Parameter sensitivity analysis yields a raw “cell sensitivity” metric which computes the responsiveness of Cell Growth to change in a selected parameter. The Cell Sensitivity calculation can be broadly simplified into two steps. First, the partial derivative of cell growth with respect to the selected parameter is taken, and it is evaluated at all time points spanning the 48 hour model simulation. Second, the absolute values of the partial derivative evaluations are added together. This final sum is directly proportional to the Cell Sensitivity for that parameter:

$$\sum_{n=0}^{48} \left| \frac{\partial \text{Cell Growth}}{\partial \text{Parameter}} \Big|_{t=n} \right| \propto \text{Cell Sensitivity}$$

More specifically, to compute the Cell Sensitivity of a parameter, the partial derivative of Cell Growth with respect to that parameter is taken at all time points from 0-48 hours (simulation time period of all models). A curve is then produced from the set of (time, calculated partial derivative) values. The magnitude of the integral of this curve is the overall Cell Sensitivity for the selected parameter. The absolute value of the integral is taken so the influence of a parameter which positively affects cell growth (elicits positive Cell Growth partial derivative values) is treated the same as the influence of parameter which negatively affects cell growth (elicits negative Cell Growth partial derivative values).

To identify how stromal fibroblasts differentially helped aid the growth of only BT 474, parameter sensitivity analysis was run on all four ODE model variants (BT 474/HCC 1954 Monoculture & Co-culture) using MATLAB’s SimBiology toolbox. Parameter sensitivity analysis was run with respect to two key PI3K/Akt pathway pro-growth signaling mechanisms:

1. pHER2 Catalysis - The rate at which the pHER2 protein enzymatically activates the Akt protein into its pAkt variant.
2. pAkt Catalysis - The rate at which the pAkt protein enzymatically activates the S6 protein into its pS6 variant.

BT 474 Sensitivity to PI3k/Akt Pro-Growth Signaling under Monoculture & Co-culture

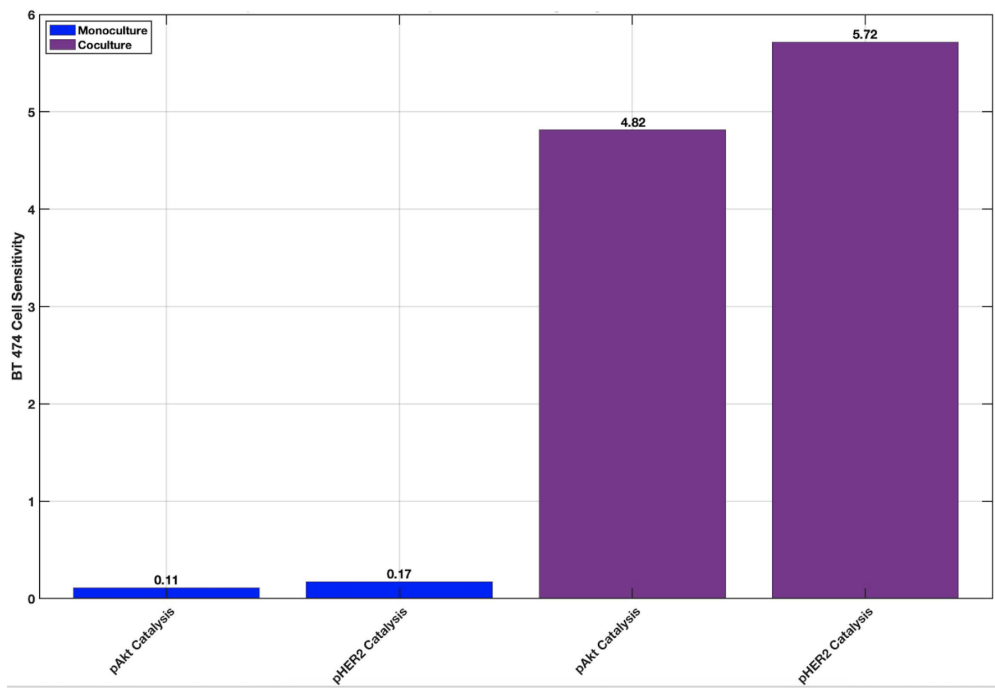


Figure 9: Once BT 474 cells are co-cultured with stromal fibroblasts (purple bars), cell sensitivity to PI3K/Akt pathway pro-growth signaling mechanisms increases dramatically.

HCC 1954 Sensitivity to PI3k/Akt Pro-Growth Signaling under Monoculture & Co-culture

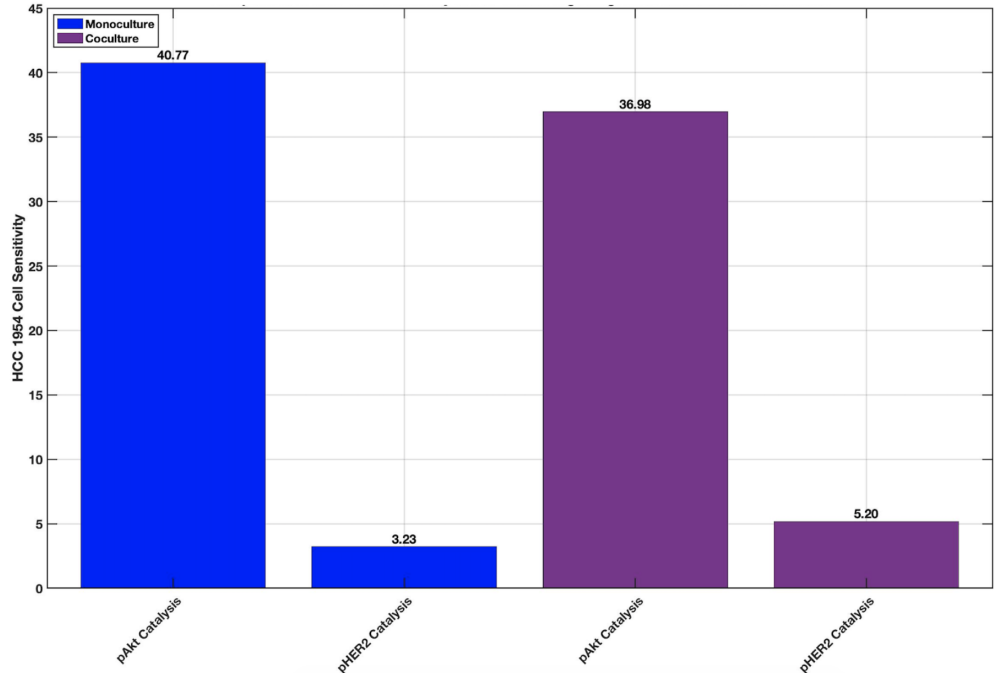


Figure 10: HCC 1954 cell sensitivity to PI3K/Akt pathway pro-growth signaling mechanisms is relatively unaffected by stromal fibroblast co-culture.

In the Fibroblast-protected BT 474 cell line, Fibroblast Co-culture dramatically increased cell sensitivity to pro-growth PI3k/Akt pathway signaling. In Monoculture, the sum of BT 474 cell sensitivity to pHER2 and pAkt Catalysis was 0.28. In Fibroblast Co-culture, the sum of BT 474 cell sensitivity to pHER2 and pAkt Catalysis was 10.54. This 3664.29% increase in net BT 474 cell sensitivity to pro-growth PI3k/Akt pathway signaling resulted solely from the influence of stromal fibroblasts.

While Fibroblast Co-culture caused a dramatic shift in BT 474 cell sensitivity to pro-growth PI3k/Akt pathway signaling, no such shift was observed in the fibroblast-insensitive HCC 1954 cell line. In Monoculture, the sum of HCC 1954 cell sensitivity to pHER2 and pAkt Catalysis was 44. In Fibroblast Co-culture, the sum of HCC 1954 cell sensitivity to pHER2 and pAkt Catalysis was 42.18. This -4.14% decrease in net HCC 1954 cell sensitivity to pro-growth PI3k/Akt pathway signaling indicates fibroblasts imparted a negligible influence on cell growth.

These results indicate that for fibroblast-protected cell lines, Fibroblast Co-culture is able to differentially promote cell growth in the face of Lapatinib assault by directly increasing cell sensitivity to pro-growth signaling mechanisms of the PI3K/Akt pathway. This stromal fibroblast boon to cell growth thereby results in Lapatinib resistance.

Combination Drug Simulations Reproduce Previously Published Findings

The power of computational cell modeling is twofold. Not only can model parameters be analyzed to yield fundamental understanding of biologically complex systems, but models can also be easily extended to simulate how combination drug therapies will arrest cell growth. Since the BT 474 and HCC 1954 ODE models had been fit and could accurately replicate observed 48 hour PI3K/Akt pathway protein dynamics and overall cell growth, the models were extended to simulate how combination drug therapies would arrest cell growth.

To validate model drug simulations, the previously published findings of (Korkola et al., 2015) were utilized. It was reported that when a pAkt inhibitor was introduced in tandem with Lapatinib, the two drugs synergized to elicit a cytotoxic effect only in cell lines which possessed a strong gain-of-function PI3K mutation. Since HCC 1954 possessed a strong gain-of-function PI3K mutation and BT 474 did not, if the models were calibrated correctly, a simulated Lapatinib + pAkt Inhibitor drug combination would only yield a cytotoxic effect in HCC 1954.

To ensure drug simulations were as biologically realistic as possible, the Fibroblast Co-culture BT 474/HCC 1954 ODE models were utilized. For both BT 474/HCC 1954, models were simulated to predict 48 hour cell growth under four different conditions:

1. DMSO Control (No Drug)
2. Lapatinib
3. pAkt Inhibitor
4. Lapatinib + pAkt Inhibitor

It should be noted the mock pAkt inhibitor was constrained to exert a realistic inhibition of ~80% target pAkt protein.

Comparison of Lapatinib & pAkt Inhibitor Synergy in BT 474 vs HCC 1954

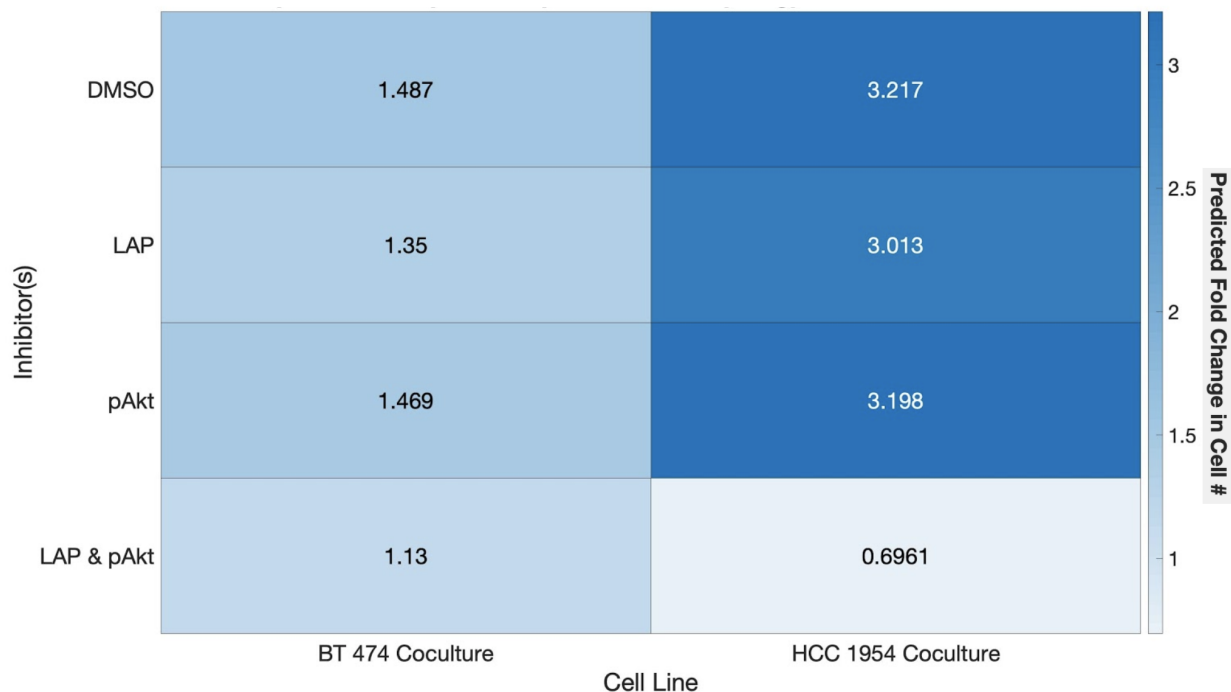


Figure 11: Heatmap Comparison of Lapatinib/ pAkt Inhibitor Drug Synergy among the PI3K wild type BT 474 & PI3K mutant HCC 1954 models. Heatmap “Temperature” is predicted fold change in cell number with respect to the initial cell number at hour 0.

The temperature of the heatmap is the model-predicted Fold Change in Cell Number after 48 hours of growth. Predicted Fold Change in Cell Number is calculated by the following equation:

$$\text{Predicted Fold Change in Cell Number} = \frac{\text{Predicted 48 Hour Cell Number}}{\text{Initial Cell Number}}$$

The Lapatininib + pAkt Inhibitor drug combination produced a Predicted Fold Change in Cell Number greater than 1 in the BT 474 model (1.13), but less than 1 in the HCC 1954 model (0.6961). Thus, the ODE models correctly predicted that the Lapatininib + pAkt Inhibitor drug combination would only cause death in the PI3K mutant HCC 1954 cells. By reproducing the findings of (Korkola et al., 2015) these drug combination simulations validated the formulation and calibration of both the BT 474 and HCC 1954 ODE models.

Triple Combination Drug Therapies may be the Best Means to Stall the Growth of Fibroblast-Protected Cell Lines such as BT 474

BT 474 is fibroblast-protected from Lapatininib. While in isolation Lapatininib can effectively stall BT 474 cell growth, in the presence of stromal fibroblasts BT 474 cells become resistant to Lapatininib. Since drug simulations using the BT 474 Fibroblast Co-culture ODE model had been validated against the findings of (Korkola et al., 2015), the model was utilized to investigate optimal means of arresting BT 474 cell growth.

Three different drug combinations were simulated under varying potencies:

1. Lapatinib + pAkt Inhibitor
2. Lapatinib + Fibroblast Signaling Inhibitor
3. Lapatinib + pAkt Inhibitor + Fibroblast Signaling Inhibitor

Predicted BT 474 Cell Viabilities Under Different Combination Therapies (Co-culture)

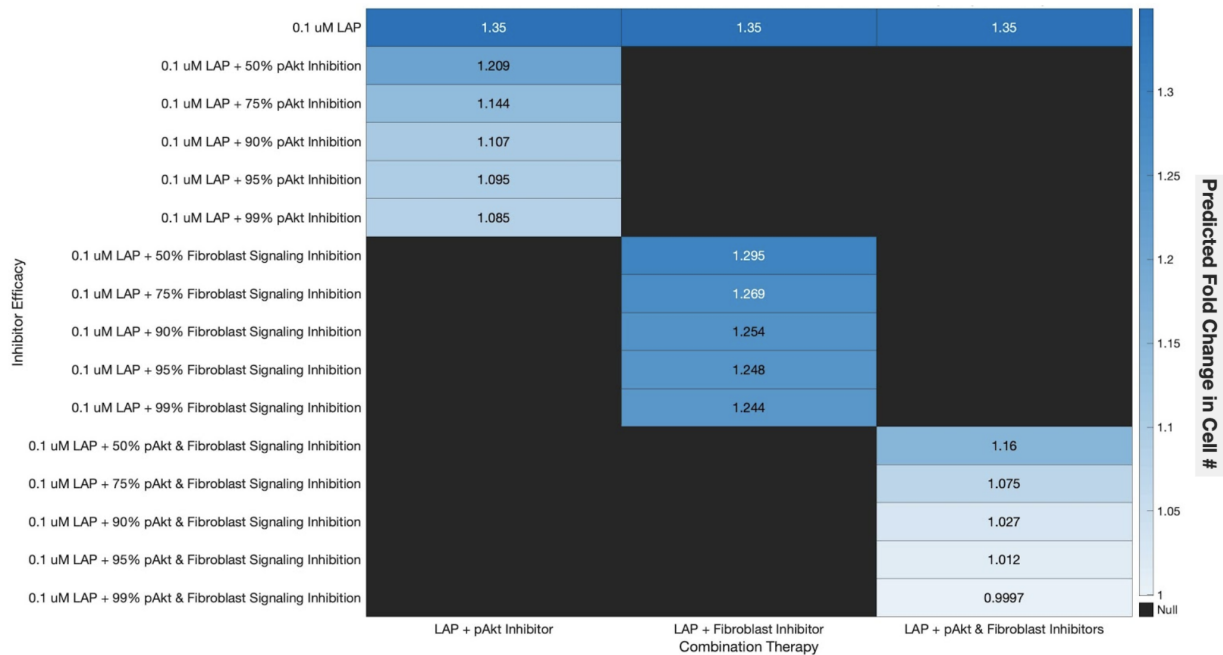


Figure 12: Heatmap Comparison of various drug combination therapies acting upon the Co-culture BT 474 cell line model. Heatmap “Temperature” is predicted fold change in cell number with respect to the initial cell number at hour 0.

Heatmap analysis leads to the conclusion the most effective means to arrest cell growth in the fibroblast-protected BT 474 cell line is to utilize Lapatinib, a pAkt Inhibitor, and a Fibroblast Signaling Inhibitor. Lapatinib & 99% inhibition of pAkt yields a relative cytostatic response (1.085 fold change in Cell Number). Lapatinib & 99% inhibition of Fibroblast Signaling yields continued cell growth (1.244 fold change in Cell Number). Lapatinib, combined with pAkt and Fibroblast Signaling Inhibitors of 99% efficacy, yields the best cytotoxic response (0.9997 fold change in Cell Number).

Discussion

Mathematical Modeling allows one to gain a mechanistic understanding of a complex system. In this work, Ordinary Differential Equation (ODE) models of a fibroblast-protected HER2+ Breast Cancer Cell Line (BT 474), and a fibroblast-insensitive HER2+ Breast Cancer Cell Line (HCC 1954) were generated. Model analyses have elucidated the fundamental mechanism by which stromal fibroblasts help aid the growth of fibroblast-protected HER2+ Breast Cancer cell lines in the face of Lapatinib assault. Model simulations of combination drug therapies have both reinforced prior knowledge reported by (Korkola et al., 2015), and

yielded insight into a novel triple drug combination which may effectively stall the growth of fibroblast-protected HER2+ Breast Cancer cell lines such as BT 474.

The core ODE model formulated in this work is applicable to any HER2+ Breast Cancer cell line. As long as temporal RPPA and cell growth data is provided, the ODE model can be employed to simulate the efficacy of a specified combination drug therapy. The ability to readily simulate various combination drug therapies using this ODE model offers a nontrivial boon to breast cancer research at large. Model predictions can be used in lieu of expansive “blind” cell culture drug arrays to direct in vitro experimentation. The benefit of using this computational ODE model is twofold as expansive cell culturing is financially costly, and model predictions are yielded in mere seconds.

The next step of this work is to perform in vitro BT 474 experimentation utilizing the Lapatinib + pAkt Inhibitor + Fibroblast Signaling Inhibitor drug combination. While ODE modeling indicates this combination is generally favorable, further in vitro experimentation is needed to elucidate the specific pAkt Inhibitor/Fibroblast Signaling Inhibitor concentrations and or ratios which are most cytotoxic.

This work has helped increase general knowledge about the role stromal fibroblasts play in HER2+ Breast Cancer resistance to Lapatinib. Ultimately, a complete understanding of stromal fibroblast influence will assist clinicians in administering the best drug therapies to subvert resistance.

Modeling Appendix

Lapatinib Hill Equation

$$\text{Activation}_{\text{pHER2}} = 1 - \frac{\text{Lapatinib Concentration}^{\text{Hill Coefficient}}}{\text{LapatinibIC50}^{\text{Hill Coefficient}} + \text{Lapatinib Concentration}^{\text{Hill Coefficient}}} \quad (1)$$

This Hill Equation helps modulate the activation rate of pHER2. Since the values for Lapatinib’s concentration and IC50 are known, only the Hill Coefficient parameter was fitted.

BT 474 Monoculture Model

BT 474 Monoculture Chemical Kinetic Rate Laws

$$\text{HER2}_{\text{Formation}} = \text{HER2}_{\text{FormationRate}} \quad (2)$$

This equation modulates the rate at which the HER2 protein is produced from transcription and translation of the HER2 gene. The $\text{HER2}_{\text{FormationRate}}$ parameter was fitted.

$$\text{pEHR2}_{\text{Activation}} = \text{ActivationRate}_{\text{pHER2}} * \text{HER2} \quad (3)$$

This equation modulates the rate at which the HER2 protein converts into its activate pHER2 variant. To account for Lapatinib Inhibition, the $\text{ActivationRate}_{\text{pHER2}}$ parameter is assigned the value of the $\text{DeactivationRate}_{\text{pHER2}}$ parameter multiplied by the fractional value of $\text{Activation}_{\text{pHER2}}$ ($\text{ActivationRate}_{\text{pHER2}} = \text{Activation}_{\text{pHER2}} * \text{DeactivationRate}_{\text{pHER2}}$) .

$$pEHR2_{Deactivation} = DeactivationRate_{pHER2} * pHER2 \quad (4)$$

This equation modulates the rate at which the pHER2 protein converts into its inactive HER2 variant. The $DeactivationRate_{pHER2}$ parameter was fitted.

$$HER2_{Degradation} = HER2_{DegradationRate} * HER2 \quad (5)$$

This equation modulates the rate at which the HER2 protein is degraded. The $HER2_{DegradationRate}$ parameter was fitted.

$$Akt_{Formation} = Akt_{FormationRate} \quad (6)$$

This equation modulates the rate at which the Akt protein is produced from transcription and translation of the Akt1 gene. The $Akt_{FormationRate}$ parameter was fitted.

$$pAktActivation_{pHER2} = \frac{kcat_{pHER2} * pHER2 * Akt}{km_{Akt_{pHER2}} + Akt} \quad (7)$$

This equation modulates the rate at which the pHER2 protein enzymatically activates the Akt protein into its pAkt variant. The $kcat_{pHER2}$ and $km_{Akt_{pHER2}}$ parameters were fitted. Michaelis-Menten kinetics were assumed.

$$pAktDeactivation = \frac{kcat_{PTEN} * PTEN * pAkt}{km_{pAkt} + pAkt} \quad (8)$$

This equation modulates the rate at which the PTEN protein enzymatically deactivates the pAkt protein into its Akt variant. The $kcat_{PTEN}$ and km_{pAkt} parameters were fitted. Michaelis-Menten kinetics were assumed.

$$Akt_{Degradation} = Akt_{DegradationRate} * Akt \quad (9)$$

This equation modulates the rate at which the Akt protein is degraded. The $Akt_{DegradationRate}$ parameter was fitted.

$$PTEN_{Formation} = PTEN_{FormationRate} \quad (10)$$

This equation modulates the rate at which the PTEN protein is produced from transcription and translation of the PTEN gene. The $PTEN_{FormationRate}$ parameter was fitted.

$$PTEN_{Degradation} = PTEN_{DegradationRate} * PTEN \quad (11)$$

This equation modulates the rate at which the PTEN protein is degraded. The $PTEN_{DegradationRate}$ parameter was fitted.

$$S6_{Formation} = S6_{FormationRate} \quad (12)$$

This equation modulates the rate at which the S6 protein is produced from transcription and translation of the RPS6 gene. The $S6_{FormationRate}$ parameter was fitted.

$$pS6Activation_{pAkt} = \frac{kcat_{pAkt} * pAkt * S6}{km_{S6pAkt} + S6} \quad (13)$$

This equation modulates the rate at which the pAkt protein enzymatically activates the S6 protein into its pS6 variant. The $kcat_{pAkt}$ and km_{S6pAkt} parameters were fitted. Michaelis-Menten kinetics were assumed.

$$pS6Regulation = pS6RegulationRate * pS6 \quad (14)$$

This equation modulates the rate at which the pS6 protein is converted back into its inactive S6 variant. The $pS6RegulationRate$ parameter was fitted.

$$S6Degradation = S6DegradationRate * S6 \quad (15)$$

This equation modulates the rate at which the S6 protein is degraded. The $S6DegradationRate$ parameter was fitted.

BT 474 Monoculture Ordinary Differential Equations

$$\frac{dHER2}{dt} = HER2_{Formation} + pEHR2_{Deactivation} - HER2_{Degradation} - pEHR2_{Activation} \quad (16)$$

The rate of change of HER2 protein concentration is equivalent to the net difference between the rate at which HER2 is formed from gene transcription and pHER2 deactivation, and the rate at which HER2 is lost to degradation and pHER2 activation.

$$\frac{dpHER2}{dt} = pEHR2_{Activation} - pEHR2_{Deactivation} \quad (17)$$

The rate of change of the pHER2 protein concentration is equivalent to the net difference between the rate HER2 activates into pHER2, and the rate at which pHER2 deactivates into HER2.

$$\frac{dAkt}{dt} = Akt_{Formation} + pAkt_{Deactivation} - Akt_{Degradation} - pAktActivation_{pHER2} \quad (18)$$

The rate of change of Akt protein concentration is equivalent to the net difference between the rate at which Akt is formed from gene transcription and pAkt deactivation, and the rate at which Akt is lost to degradation and pAkt activation by pHER2.

$$\frac{dpAkt}{dt} = pAktActivation_{pHER2} - pAkt_{Deactivation} \quad (19)$$

The rate of change of the pAkt protein concentration is equivalent to the net difference between the rate at which HER2 activates Akt into pAkt, and the rate at which PTEN deactivates pAkt into Akt.

$$\frac{dPTEN}{dt} = PTEN_{Formation} - PTEN_{Degradation} \quad (20)$$

The rate of change of the PTEN protein concentration is equivalent to the net difference of the rate at which PTEN is formed from gene transcription, and the rate at which PTEN is lost to degradation.

$$\frac{dS6}{dt} = S6_{Formation} + pS6_{Regulation} - S6_{Degradation} - pS6Activation_{pAkt} \quad (21)$$

The rate of change of S6 protein concentration is equivalent to the net difference between the rate at

which S6 is formed from gene transcription and pS6 regulation, and the rate at which S6 is lost to degradation and pS6 activation by pAkt.

$$\frac{dpS6}{dt} = pS6\text{Activation}_{pAkt} - pS6\text{Regulation} \quad (22)$$

The rate of change of the pS6 protein concentration is equivalent to the net difference between the rate S6 is activated into pS6 by pAkt, and the rate at which pS6 deactivates into S6.

$$\frac{d\text{Cells}}{dt} = \text{TimeDelay} * \text{Cells} * (\text{pS6} - \text{Threshold}) \quad (23)$$

The rate of Change of cells is proportional to the difference between the level of pS6 protein concentration and a fitted Threshold parameter. The Threshold parameter is included to model how cell death will occur if pS6 protein concentration is low. A TimeDelay parameter is included to connect faster intracellular PI3k/Akt signaling to slower overall cell growth.

HCC 1954 Monoculture Model

HCC 1954 only differs from BT 474 in that it possesses a strong gain-of-function PI3K protein mutation. To account for this PI3K protein mutation aiding HCC 1954 cell growth, a mechanism of PI3K-modulated pAkt protein activation is incorporated.

HCC 1954 Monoculture Chemical Kinetic Rate Laws

The core chemical kinetic rate laws described in equations 2-15 from the BT 474 Monoculture model are held in the HCC 1954 Monoculture model. The only additional chemical kinetic rate law describes PI3K-modulated activation of the pAkt protein:

$$pAkt\text{Activation}_{PI3KMutant} = \frac{k_{cat,PI3KMutant} * PI3KMutant * Akt}{km_{Akt,PI3KMutant} + Akt} \quad (24)$$

This equation modulates the rate at which the mutant PI3K protein enzymatically activates the Akt protein into its pAkt variant. The $k_{cat,PI3KMutant}$ and $km_{Akt,PI3KMutant}$ parameters were fitted. Michaelis-Menten kinetics were assumed.

HCC 1954 Monoculture Ordinary Differential Equations

HCC 1954 only differs from the BT 474 in that HCC 1954 possesses a strong gain-of-function PI3K protein mutation. The similarities between HCC 1954 and BT 474 are reflected in the overlap of their Monoculture model ODEs. The core ODEs described in equations 16-17 and 20-23 in the BT 474 Monoculture model were maintained in the HCC 1954 Monoculture model. Only the Akt/pAkt ODEs described in equations 18-19 are adjusted to reflect the influence of the mutant PI3K protein.

$$\frac{dAkt}{dt} = Akt_{Formation} + pAkt_{Deactivation} - Akt_{Degradation} - pAkt\text{Activation}_{pHER2} - pAkt\text{Activation}_{PI3KMutant} \quad (25)$$

The rate of change of Akt protein concentration is equivalent to the net difference between the rate at which Akt is formed from gene transcription and pAkt deactivation, and the rate at which Akt is lost to degradation and pAkt activation from the HER2 and mutant PI3k proteins.

$$\frac{dpAkt}{dt} = pAktActivation_{pHER2} + pAktActivation_{PI3KMutant} - pAktDeactivation \quad (26)$$

The rate of change of the pAkt protein concentration is equivalent to the net difference between the rate at which the HER2 and mutant PI3K proteins activate Akt into pAkt, and the rate at which PTEN deactivates pAkt into Akt.

BT 474 & HCC 1954 Co-culture Model

For both BT 474 and HCC 1954, the only difference between the Monoculture and stromal fibroblast Co-culture models is presence of stromal fibroblasts. In accordance with the findings of (Zervantonakis et al., 2020), to model stromal fibroblast-influence on overall BT 474/HCC 1954 cell growth, a fibroblast means of pS6 activation is incorporated.

BT 474 & HCC 1954 Co-culture Chemical Kinetic Rate Laws

For BT 474, the core chemical kinetic rate laws described in equations 2-15 are preserved. For HCC 1954, the core chemical kinetic rate laws described in equations 2-15 & 24 are preserved. The only additional equation added for both models describes fibroblast-mediated pS6 activation:

$$pS6Activation_{Fibroblasts} = \frac{kcat_{Fibroblasts} * Fibroblasts * S6}{km_{S6Fibroblasts} + S6} \quad (27)$$

This equation modulates the rate at which stromal fibroblasts enzymatically activate the S6 protein into its pS6 variant. The $kcat_{Fibroblasts}$ and $km_{S6Fibroblasts}$ parameters were fitted. Michaelis-Menten kinetics were assumed.

BT 474 & HCC 1954 Co-culture Ordinary Differential Equations

For BT 474, the core ODEs described in equations 16-20 and 23 are preserved. For HCC 1954, the core ODEs described in equations 16-17, 20, 25-26, and 23 are preserved. Only the S6/pS6 ODEs were adjusted across both models to reflect the influence of stromal fibroblasts:

$$\frac{dS6}{dt} = S6_{Formation} + pS6_{Regulation} - S6_{Degradation} - pS6Activation_{pAkt} - pS6Activation_{Fibroblasts} \quad (28)$$

The rate of change of S6 protein concentration is equivalent to the net difference between the rate at which S6 is formed from gene transcription and pS6 regulation, and the rate at which S6 is lost to degradation and pS6 activation from both pAkt and Fibroblasts.

$$\frac{dpS6}{dt} = pS6Activation_{pAkt} + pS6Activation_{Fibroblasts} - pS6Regulation \quad (29)$$

The rate of change of the pS6 protein concentration is equivalent to the net difference between the rate at which S6 is activated into pS6 via enzymatic action from pAkt and Fibroblasts, and the rate at which pS6 deactivates into S6.

Optimized Model Parameters

Table 1: Values of Optimized Parameter Values across all ODE Model Variants

| Parameter | Model Variant | | | |
|---|---------------|--------------|----------|---------------|
| | BT Mono | BT Fibro Co. | HCC Mono | HCC Fibro Co. |
| Hill Coefficient | 0.283 | 0.35 | 0.68 | 1.00 |
| HER2FormationRate | 11.82 | 3.74 | 1.13 | 1.00 |
| ActivationRate _{pHER2} | 3.27 | 0.30 | 0.15 | 0.09 |
| DeactivationRate _{pHER2} | 9.46 | 0.96 | 0.85 | 1.01 |
| HER2DegradationRate | 7.28 | 1.00 | 0.26 | 1.00 |
| AktFormationRate | 7.57 | 5.07 | 4.90 | 1.02 |
| kcat _{pHER2} | 6.98 | 3.23 | 0.21 | 0.99 |
| km _{Akt} _{pHER2} | 0.23 | 0.41 | 1.88 | 1.01 |
| kcat _{PI3KMutant} | n/a | n/a | 1.63 | 1.02 |
| km _{Akt} _{PI3KMutant} | n/a | n/a | 0.35 | 0.99 |
| kcat _{PTEN} | 8.20 | 16.44 | 3.41 | 0.99 |
| km _{pAkt} | 1.16 | 3.68 | 0.29 | 1.01 |
| AktDegradationRate | 2.12 | 1.03 | 2.12 | 0.99 |
| PTENFormationRate | 3.44 | 3.66 | 0.33 | 0.98 |
| PTENDegradationRate | 2.75 | 2.93 | 0.40 | 1.01 |
| S6FormationRate | 0.19 | 0.55 | 5.56 | 1.07 |
| kcat _{pAkt} | 0.50 | 1.36 | 3.77 | 1.06 |
| km _{S6pAkt} | 0.43 | 0.78 | 0.30 | 0.96 |
| kcat _{Fibroblasts} | n/a | 0.55 | n/a | 1.07 |
| km _{S6Fibroblasts} | n/a | 1.27 | n/a | 0.96 |
| pS6RegulationRate | 1.98 | 0.85 | 1.13 | 0.91 |
| S6DegradationRate | 0.30 | 5.73 | 1.10 | 0.95 |
| TimeDelay | 1.2E-3 | 3.9E-2 | 2.5E-2 | 5.0E-2 |
| Threshold | 2.75 | 1.8E-3 | 0.45 | 0.90 |

References

- Carey, L. A., Berry, D. A., Cirrincione, C. T., Barry, W. T., Pitcher, B. N., Harris, L. N., ... Weckstein, D. J. e. a. (2016). Molecular heterogeneity and response to neoadjuvant human epidermal growth factor receptor 2 targeting in calgb 40601, a randomized phase iii trial of paclitaxel plus trastuzumab with or without lapatinib. *Journal of Clinical Oncology, 34*(6), 542-549. doi: 10.1200/jco.2015.62.1268
- Dufner, A., & Thomas, G. (1999). Ribosomal s6 kinase signaling and the control of translation. *Experimental Cell Research, 253*(1), 100-109. Retrieved from <https://www.sciencedirect.com/science/article/pii/S0014482799946839?via%3Dihub> doi: 10.1006/excr.1999.4683
- Gagliato, D. M., Jardim, D. F., Marchesi, M. P., & Hortobagyi, G. (2016). Mechanisms of resistance and sensitivity to anti-her2 therapies in her2+ breast cancer. *Oncotarget, 7*(39), 64431-64446. Retrieved from <https://www.oncotarget.com/article/7043/> doi: <https://doi.org/10.18632/oncotarget.7043>
- Her2 and targeted therapy.* (2020). Retrieved from <https://www.smartpatients.com/targets/her2>
- Kirouac, D. C., Schaefer, G., Chan, J., Merchant, M., Orr, C., Huang, S.-M. A., ... et al. (2017, Jun). Clinical responses to erk inhibition in braf v600e -mutant colorectal cancer predicted using a computational model. *Nature News.* Retrieved from <https://www.nature.com/articles/s41540-017-0016-1>
- Korkola, J. E., Collisson, E. A., Heiser, L., Oates, C., Bayani, N., Itani, S., ... Wang, N. J. e. a. (2015). Decoupling of the pi3k pathway via mutation necessitates combinatorial treatment in her2+ breast cancer. *PLOS ONE, 10*(7), e0133219. doi: 10.1371/journal.pone.0133219
- Liu, L., Liu, L., Yao, H. H., Zhu, Z. Q., Ning, Z. L., & Huang, Q. (2016, May). Stromal myofibroblasts are associated with poor prognosis in solid cancers: A meta-analysis of published studies. *Plos One, 11*(7). Retrieved from <https://www.ncbi.nlm.nih.gov/pmc/articles/PMC4961396/> doi: 10.1371/journal.pone.0159947
- Paplomata, E., & O'Regan, R. (2014, Jul). *The pi3k/akt/mTOR pathway in breast cancer: targets, trials and biomarkers.* SAGE Publications. Retrieved from <https://www.ncbi.nlm.nih.gov/pmc/articles/PMC4107712/>
- Zervantonakis, I. K., Poskus, M. D., Scott, A. L., Selfors, L. M., Lin, J.-R., Dillon, D. A., ... Brugge, J. S. (2020). Fibroblast–tumor cell signaling limits her2 kinase therapy response via activation of mTOR and antiapoptotic pathways. *Proceedings of the National Academy of Sciences, 117*(28), 16500–16508. Retrieved from <https://www.pnas.org/content/117/28/16500> doi: 10.1073/pnas.2000648117